Journal of Holistic Integrative Pharmacy 5 (2024) 149–156

Contents lists available at ScienceDirect

Journal of Holistic Integrative Pharmacy

journal homepage: www.keaipublishing.com/en/journals/journal-of-holistic-integrative-pharmacy

Preparation of purine functionalized biochar and analysis of nephrotoxic substances in traditional Chinese medicine

Yanhui Ge [a,b,*], Xinya Xu [c], Yuanru Zheng [a]

[a] School of Pharmacy, Guangdong Pharmaceutical University, Guangzhou, 510006, China
[b] The First Affiliated Hospital, Guangdong Pharmaceutical University, Guangzhou, 510000, China
[c] School of Pharmacy, Shaanxi University of Chinese Medicine, Xianyang, 712000, China

ARTICLE INFO

Keywords:
Biochar
Purine functionalized materials
Nephrotoxic substances
Traditional Chinese medicine

ABSTRACT

In recent years, a growing lack of comprehension regarding the safety of traditional Chinese medicines (TCMs) has led to an escalating incidence of drug-induced organ damage, particularly kidney damage associated with TCM usage. This study focused on the development of purine-functionalized biochar and used to capture nephrotoxic substances in TCMs. The biochar was meticulously characterized using scanning electron microscopy (SEM), Fourier-transform infrared spectroscopy (FT-IR), X-ray photoelectron spectroscopy (XPS) and elemental analysis. Subsequently, it was employed as a solid-phase extraction medium for capturing suspected nephrotoxic substances in TCMs. Results revealed that the functional biochar exhibited commendable selectivity for compounds with nephrotoxic effects, demonstrating its potential for effectively capturing nephrotoxic substances in TCMs. This research aimed to introduce an innovative method for monitoring potential nephrotoxic substances in large-scale TCMs, thereby contributing to the enhancement of the overall safety profile of traditional Chinese medicine.

1. Introduction

In recent years, traditional Chinese medicine (TCM) has demonstrated distinctive efficacy in treating specific advantageous diseases, gaining increased recognition worldwide as a supplementary and alternative medical option. Simultaneously, the safety issues associated with TCM have become more pronounced.[1–3] Insufficient understanding of the safety issues has led to a rise in incidents of drug-induced organ damage, particularly due to self-administration, indiscriminate use, prolonged usage and excessive consumption of TCM. Kidney damage, in particular, has emerged as a significant concern associated with the use of TCM. The intricate chemical composition of TCM posed a substantial challenge in studying its toxicity.[4,5] Nevertheless, as TCMs has widespread application and undergoes in-depth research, scholars have increasingly focused on its nephrotoxicity. Ensuring the safety of the clinical application of TCM has become an urgent matter that required immediate attention.

Presently, the preclinical methods employed for assessing the nephrotoxicity of TCM primarily involved both animal experiments and cell line model. The existing literature outlined three main models. The first was the animal model of diabetic nephropathy using streptozotocin and alloxan[6]; The second were adriamycin nephropathy models, encompassing microvascular nephropathy and focal segmental glomerulosclerosis models[7]; The third was in vitro cultivation of rat mesangial cell lines,[8] with the dynamic observation of mesangial cell proliferation at different time in each group under the influence of drug-containing serum using thiazole blue colorimetry. Both glomerular mesangial cell line experiments and animal experiments were commonly utilized for evaluating drug safety. However, employing experimental animal pathology and related biochemical indicators for renal toxicity evaluation presented several challenges up to now. These included difficulties in controlling experimental design, the potential for false negatives or false positives, and the relatively independent nature of toxic component analysis and toxicity evaluation. This independence lead to issues such as large scale of training sample, prolonged experimental durations, extensive workloads and diminished evaluation efficiency in animal experiments. There was a pressing need to establish a new analytical method capable of swiftly identifying toxic components responsible for nephropathy in TCM, addressing the limitations associated with current evaluation approaches.

Various theories have been proposed to elucidate the mechanisms of drug-induced nephrotoxicity,[9,10] with one notable theory focusing on the

* Corresponding author. School of Pharmacy, Guangdong Pharmaceutical University, Guangzhou, 510006, China.
E-mail addresses: geyanhui@gdpu.edu.cn, geyanhui618@163.com (Y. Ge).

https://doi.org/10.1016/j.jhip.2024.06.006
Received 24 April 2024; Received in revised form 6 June 2024; Accepted 18 June 2024

formation of adducts between chemical components and DNA bases within the cell nucleus. An illustrative example involves the metabolic mechanism of toxic pyrrolizidine alkaloids (PAs) in vivo, which comprised two primary aspects: first, PAs binded with hemoglobin, which leads to the formation of dehydroalkaloid hemoglobin adducts and subsequent cytotoxicity.[11] Seccond, PAs combined with DNA base in the nucleus of liver sinusoidal endothelial cells, resulting in the formation of dehydroalkaloid DNA adducts and causing genetic toxicity.[12] Research has demonstrated that these adducts could serve dual roles. Firstly, they could act as biomarkers, reflecting the concentration of hepatotoxic substances in vivo. Additionally, they functioned as effector markers, providing insights into the effective dose of hepatotoxic substances reaching target organs.[13] This perspective highlighted the potential utility of adduct formation as a valuable indicator in assessing the impact of toxic substances on the liver.

Currently, various methods were employed for screening nephrotoxic substances. The first was the use of fluorescent probes,[14] this method utilized specialized dyes emitting fluorescence upon interaction with specific substances, facilitating the identification of nephrotoxic components. The second was based on mathematical models,[15] these models analyzed various parameters and relationships, serving as a predictive tool for assessing the potential nephrotoxicity of specific components. The third was conducted using biochip technology,[16] which was equipped with specific probes or sensors, enabled the detection and identification of nephrotoxic agents, contributing to efficient screening processes. The fourth was high content analysis (HCA).[17] HCA automated the imaging and analysis of a large number of cells or samples, allowing for the simultaneous assessment of multiple parameters related to nephrotoxicity. These diverse screening methods provided complementary approaches, offering a comprehensive toolkit for identifying and evaluating nephrotoxic substances in TCMs.

Natural biochar possessed several advantageous characteristics, including heat resistance, pressure resistance, acid and alkali resistance and good conductivity. Furthermore, the biochar surface exhibited active groups such as hydroxyl, carboxyl, and phenolic hydroxyl. These performance enabled biochar to effectively adsorb environmental pollutants in soil and water, rendering it a valuable natural adsorbent. Owing to its exceptional physical and chemical properties, biochar has garnered increasing attention from scientists and was currently experiencing rapid development in the field of sample pretreatment.[18,19] In Shu's work, hybrid-type carbon derived from zucchini (*Cucurbita pepo* L.) was utilized for the extraction of aristolochic acid I from *Aristolochiaceae* medicinal plants,[20] demonstrating satisfactory selectivity. Ge's research involved the fabrication of magnetic porous biochar from *pericarpium granati*, which was employed as an adsorbent for aristolochic acids in rat urine.[21] Additionally, Ge's team employed shrimp shell-derived magnetic FeNi biochar for the specific recognition of monocrotaline in herbal medicine.[22]

In this study, *Glycyrrhiza uralensis* Fisch was employed as the source and subjected to high-temperature carbonization to obtain biochar. Building upon the theory that nephrotoxic substances can form adducts with DNA bases, our proposal involved grafting purine bases onto biochar. These modified materials served as a packed solid-phase extraction adsorbent, combined with high-performance liquid chromatography (HPLC) technology, and then it was utilized to capture components in TCMs. The ultimate goal was to establish a detection method for capturing nephrotoxic components in TCMs and traditional Chinese patent medicines.

2. Experiment

2.1. Materials and chemicals

2′-deoxyguanosine hydrate, 2′-deoxyadenosine, naproxen, indomethacin, berberine, hydrochloride clenbuterol, enodin, ofloxacin, AAs (a mixture of AAI and AAII), indomethacin (99%) were obtained from Shanghai Aladdin Biochemical Technology Co., Ltd. HPLC-grade acetonitrile and methanol were purchased from Tianjin Kemiou Chemical Reagent Co. (Tianjin, China). *Glycyrrhiza uralensis* Fisch. (dry roots and rhizomes). *Coptis chinensis* Franch. (rhizome), *Aristolochia mollissima* Hance (above ground), *Citrus reticulata* Blanco (dry and ripe fruit peel) were purchased from a local herb store. The TCMs were milled and passed through a 40-mesh sieve. Ultrapure water was prepared by using Molement 1805b purification system (Shanghai, China). All other chemicals were analytical reagent grade and provided by local suppliers. Solid phase extration (SPE) empty column (4.5 mL) was brought from Shenzhen Dudian Biotechnology Co., Ltd.. Penicillin sodium (> 97%) was purchased from Xi'an Renda Biotechnology Co., Ltd.

2.2. Preparation of TCM samples

2.2.1. Preparation of reference solution

Approximately 6.0 mg of aristolochic acid I reference substance was dissolved in methanol and subjected to sonication. The solution was then transferred to a 100 mL volumetric flask and topped up with methanol. After thorough shaking, a 60 μg/mL standard stock solution was prepared and then filtered through a 0.45 μm microporous membrane. For the AAI and AAII mixture solution, the preparation was the same in methanol as above.

2.2.2. Preparation of test solution

A total of 50.0 g of dried crude TCM powder was combined with 300 mL of 60% methanol. The mixture was subjected to heating and reflux for 2 h, followed by extraction performed thrice. The resulting filtrates were merged all. Subsequently, the combined filtrate was concentrated under vacuum using a rotary evaporator, and the concentrated solution was collected and dried in a vacuum drying oven to yield the extract. For further analysis, the extract (1.0 g) was dissolved in 5 mL of methanol. The supernatant was then filtered through a microporous membrane.

2.3. Optimization of HPLC conditions

The HPLC–UV analysis was carried out on a Shimadzu HPLC system (LC-2010AHT, Kyoto, Japan), equipped with a SPD–20A UV–vis detector and a Lab-Solution workstation. The chromatographic separation was carried out with a Promasil C_{18} column (250 mm × 4.6 mm, 5 μm) for analysis. The mobile phase was at a flow rate of 1.0 mL/min. The wavelength was set at 315 nm for detecting analytes, and a 10 μL TCM sample was injected into the HPLC-UV analytical system. The seven mobile phases were employed: methanol–acetonitrile–1% HOAc (47:17:36, v/v/v), methanol–acetonitrile–1% HOAc (40:20:40, v/v/v), methanol–0.1% HOAc (70:30, v/v), methanol–0.1% HOAc (60:40, v/v), and A phase (aqueous solution of 0.1% tetrahydrofuran and 0.1% HOAc):B phase (acetonitrile solution of 0.1% tetrahydrofuran and 0.1% HOAc) (volume ratios A:B were at 55:45, 60:40 and 62:38, v/v, respectively). These seven mobile phases were selected to determine the content of aristolochic acid I (AAI) in the same *Aristolochia mollissima* Hance spiked sample. Moreover, before the detection of AAI in TCM, the AAI standard solution was injected under the each mobile phase for positive reference.

2.4. Preparation of GCs

After the drying and crushing of *Glycyrrhiza uralensis* Fisch, the material was passed through a 200–mesh sieve, washed twice with distilled water, and then dried at 90 °C. Subsequently, 50.0 g of the resulting powder was placed in a vacuum tube furnace. The material was heated to 650 °C at a rate of 3 °C/min under a nitrogen environment, maintaining this temperature for 3 h. After cooling to room temperature, the obtained black residue was removed, washed with deionized water and anhydrous ethanol, and then dried. The final step involved crushing the material to obtain *Glycyrrhiza uralensis* Fisch carbon (GCs).

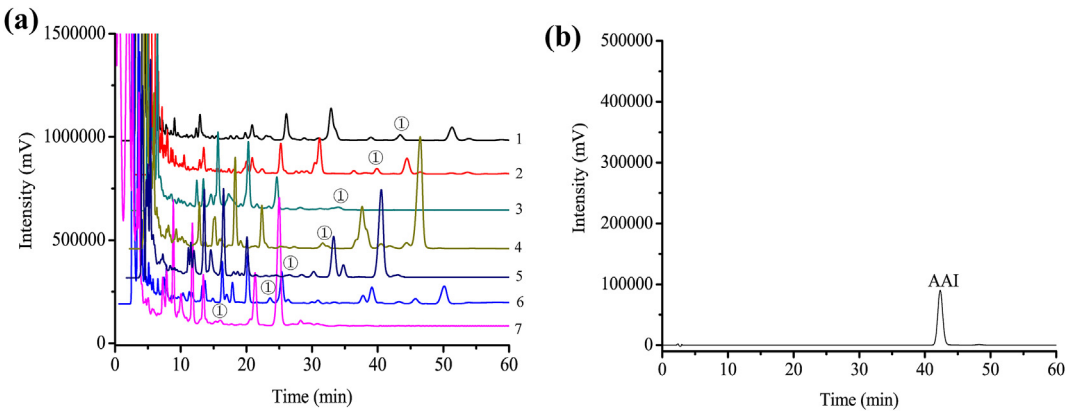

Fig. 1. (a) The chromatograms of AAI in *Asarum sieboldii* Miq. var. Seoulense, ①: AAI; (b) AAI standard solution under the mobile phase 1.
1: The volume ratio of A:B was 62:38, v/v; 2: The volume ratio of A:B was 60:40, v/v; 3: Methanol-0.1% HOAc 60:40, v/v; 4: Methanol-acetonitrile-1% HOAc 40:20:40, v/v/v; 5: Methanol-acetonitrile-1%HOAc 47:17:36, v/v/v; 6: The volume ratio of A:B was 55:45, v/v; 7: Methanol-0.1% HOAc 70:30, v/v; Phase A: (0.1% THF + 0.1% HOAc) in water; Phase B: (0.1% THF + 0.1% HOAc) in acetonitrile.

2.5. Preparation of GCs@dG

GCs (150 mg) was placed in a round-bottom flask and then add 25 mL sulfoxide chloride and 625 μL of N,N-dimethylformamide, after reacting at 70 °C for 24 h, the excess sulfoxide chloride and N,N-dimethylformamide were distilled at 90 °C to obtain the chlorinated glycyrrhizic acid material. Subsequently, N,N-dimethylformamide (25 mL), triethylamine (625 μL) and 100 mg of 2′-deoxyguanosine were added to the flask, with reacting at 130 °C for 70 h. Once the reaction was complete, the black substance was removed and washed with water for three times. Finally, GCs@dG was obtained after drying. For the synthesis of GCs@dA, all the steps were the same, only replacing 2′-deoxyguanosine with 2′-deoxyadenosine, and keeping all other conditions unchanged and follow the above steps.

2.6. Characterization of the GCs@dA and GCs@dG

SEM images were acquired using a TM-1000 scanning microscope (Hitachi, Japan). FT-IR spectra (400 - 4000 cm^{-1}) were recorded using an FT-IR-8400S spectrometer (Shimadzu, Japan). Elemental analyses (C, H, N) were carried out using an Elementar Vario EL III microanalyzer. X-ray photoelectron spectra were obtained utilizing a Nexsa X-ray photoelectron spectrometer (ThermoFisher, USA).

2.7. Selective adsorption

The selectivity of the adsorption was assessed using six compounds with different structures, including five compounds with documented

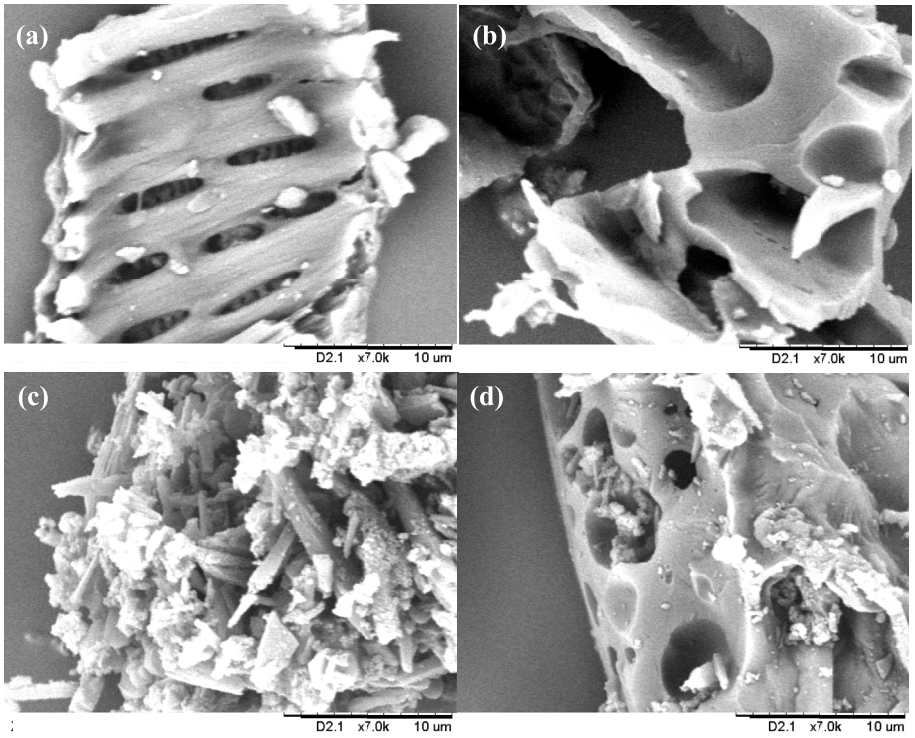

Fig. 2. The scanning electron micrographs of functionalized materials (a, b) GCs; (c) GCs@dA; (d) GCs@dG

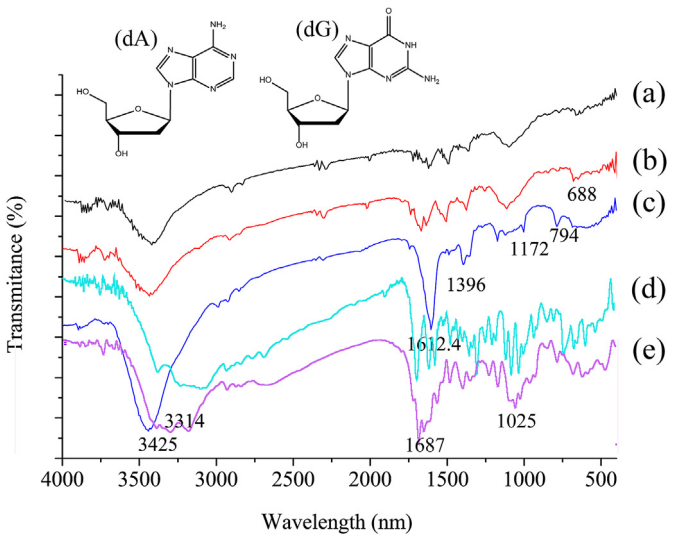

Fig. 3. The FT-IR results of functionalized biochar (a): GCs; (b): GCs@dG; (c): GCs@dA; (d): dA; (e): dG.

nephrotoxicity reported in the literature (Aristolochic acid I and II, ofloxacin, indomethacin, emodin),[23–26] and compounds without reported nephrotoxicity (penicillin sodium). Dried GCs@dA and GCs@dG (20.0 mg) were each mixed with 10 mL of aristolochic acid I and II, ofloxacin, emodin, sodium penicillin and indomethacin solutions, respectively. The mixtures were shaken for 60 min at a temperature of 25 °C. The supernatant was filtered and then the concentration of substrates were determined by HPLC to calculate the adsorption capacity (Qe) of GCs@dA and GCs@dG for each substrate using equation (1).[22] In addition, all the six compounds were detected under its own HPLC condition.

$$Q = \frac{(C_0 - C_f)V}{m} \quad (1)$$

Where C_0 (mg/L) and C_f (mg/L) were the initial and final concentrations of solute molecules, respectively, V (L) was the total volume of the solution, and m (mg) was the mass of GCs@dC and GCs@dG.

2.8. Analysis of nephrotoxic substances in TCMs

GCs@dG (100 mg) was filled into a 4.5 mL SPE empty tube. Once filled, the column was compacted under vacuum filtration. The polymer was secured on sieve plates both above and below, followed by several rinses with 2.0 mL of methanol and 2.0 mL of water. Subsequently, the TCMs sample (3.0 mL) to be tested and load it onto the column. After the sample flowing through, 3 mL of water was utilized as the washing solution. Finally, methanol acetic acid solution (3.0 mL, 9:1, v/v) was employed as the eluent. The eluent collected and evaporated under a nitrogen flow. Then the residue was dissolved in 1 mL of methanol and filtered through microporous membrane. The resulting solution was analyzed by an HPLC system to compare the differences in chromatographic peaks before and after elution.[27]

3. Results and discussion

3.1. Types and proportions of mobile phases

The content of aristolochic acid I in the test sample of *Aristolochia mollissima* Hance was determined using seven different mobile phases. The results as depicted in Fig. 1a, under a positive reference of AAI, the aristolochic acid I peak was confirm in TCM solution in each mobile phase. The optimal condition for separation, with good response and the largest peak area value, was achieved when the volume ratio of mobile phase A:B was 62:38 (Fig. 1a, 1), with a retention time of 42 min. The chromatogram of the AAI standard solution at this condition was shown in Fig. 1b. Under the condition of a 60:40 (Fig. 1a, 2), the response value of aristolochic acid I (AAI) was not as high as that under the 62:38 vol ratio condition. The use of methanol–0.1% HOAc (60:40, v/v) as the mobile phase (Fig. 1a, 3) led to a severely trailing peak shape for the target, making the detection of AAI challenging. In the case of methanol–acetonitrile–1% HOAc (40:20:40, v/v/v) (Fig. 1a, 4), the separation was poor between AAI and surrounding interfering components. Methanol–acetonitrile–1% HOAc (47:17:36, v/v/v) (Fig. 1a, 5) resulted in an extremely low peak intensity of AAI. Aristolochic acid I was not detected when the mobile phase was methanol–(0.1% HOAc) water (70:30, v/v) (Fig. 1a, 7), which was possibly due to the excessive polarity of the mobile phase causing AAI to be eluted along with interfering components, hindering the detection of the target. By adjusting the polarity of the mobile phase, the separation effect of aristolochic acid I from impurities improved. The addition of 0.1% tetrahydrofuran reduced the polarity, enhancing the retention of AAI. Most impurities could be eluted within 10 min, minimizing interference with the detection of the tested component, and resulting in better separation of AAI from interfering substances with an ideal peak shape. Therefore, the optimal mobile phase was when the volume ratio of A:B was 62:38, where phase A was 0.1% THF+0.1% HOAc aqueous solution, and phase B was an acetonitrile solution of 0.1% THF+0.1% HOAc.

3.2. Characterization of GCs@dA

In this study, *Glycyrrhiza uralensis* Fisch was utilized as a source to produce biochar, aiming to enhance the practical utility of biochar. *Glycyrrhiza uralensis* Fisch underwent chlorination at high temperature in a sulfoxide chloride solvent. Subsequently, it reacted with purine in an

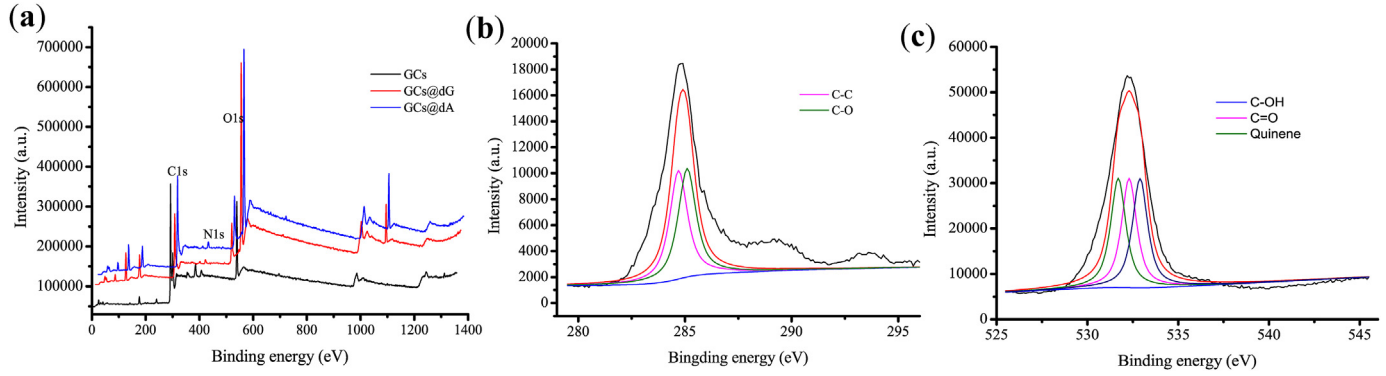

Fig. 4. (a) The X-ray photoelectron spectra of functionalized biochar; The high resolution XPS spectra C1s (b) and O1s (c) of GCs@dA

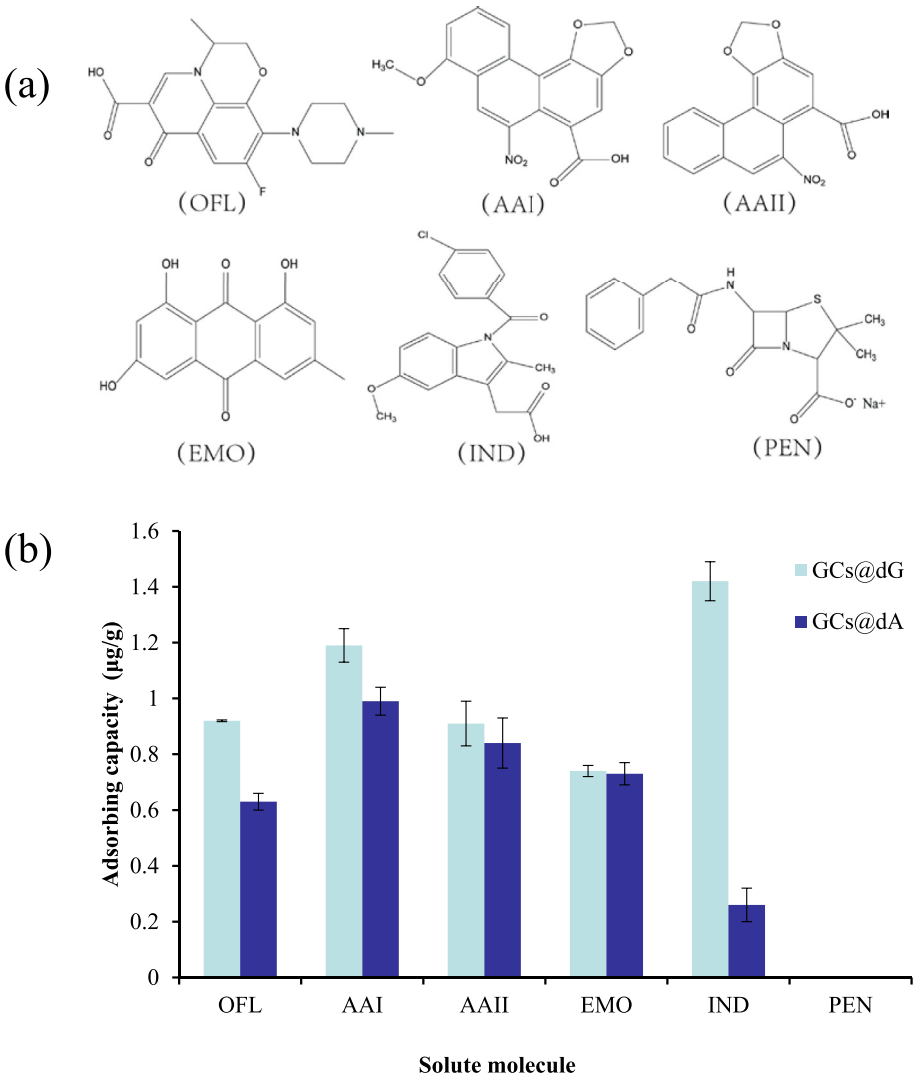

Fig. 5. (a) The structure of solute molecule; (b) The selective adsorption capacity of GCs@dA and GCs@dG (n = 3). OFL: ofloxacin; AAI: aristolochi acid I; AAII: aristolochi acid II; IND: indomethacin; EMO: emodin; PEN: penicillin sodium.

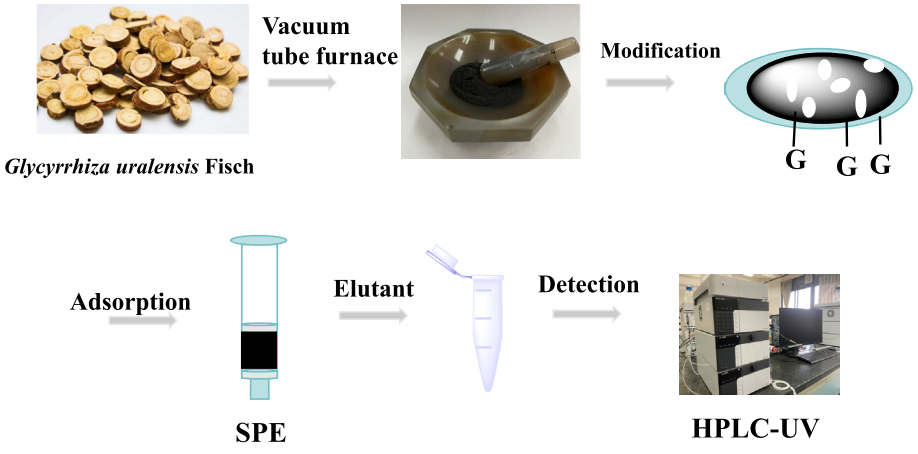

Fig. 6. The diagram of the preparation process and SPE procedure.

alkaline triethylamine environment to obtain purine-modified biochar.

3.2.1. SEM

The surface morphology of the obtained functionalized materials were depicted in Fig. 2. The results revealed that the carbon particles of GCs, exhibiting non-uniform size and possessing a porous structure, which was contributing to a larger surface area. When compared to GCs (Fig. 2a and b), both GCs@dA (Fig. 2c) and GCs@dG (Fig. 2d) exhibited

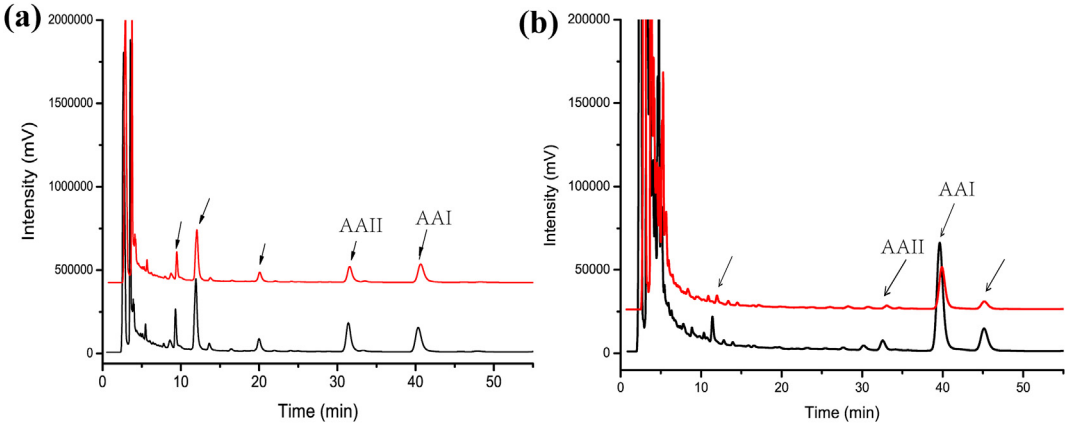

Fig. 7. The chromatogram of (a) *Aristolochia debilis* Bge. and (b) *Aristolochia mollissima* Hance. 1: after being adsorbed by GCs@dG; 2: before being adsorbed by GCs@dG; 3: chromatogram of AAI and AAII mixed standard solution; peaks marked with arrow: unknown suspected compounds.

Table 1
Elemental analysis of functionalized materials.

Samples	N%	C%	H%
GCs	4.03	73.68	2.98
GCs@dG	6.22	71.16	3.29
GCs@dA	5.54	70.63	2.51

attachments on its surface, which might be the DNA base grafting onto the biochar. The rough structure was a favorable support to illustrate the functionalization of the material.

3.2.2. *Infrared spectroscopy analysis*

Fourier transform infrared (FT-IR) spectra provided direct evidence for the deposition of the base on the surface of GCs. The obtained infrared spectrum was presented in Fig. 3. The results indicated that all five curves exhibited a broad strong peak in the range of 3100–3400 cm^{-1}, which was attributed to the vibrational peak of –OH, suggesting the presence of hydroxyl groups in GCs@dA and GCs@dG. No obvious characteristic peak of GCs was observed in Fig. 3a. Compared with GCs, GCs@dA displays two strong peaks at 1612 cm^{-1} and 1396 cm^{-1}, attributed to the stretching vibration peak of C═O in the carboxyl group, which was indicating the presence of carboxyl groups in GCs@dA. Additionally, both GCs@dA and GCs@dG exhibited similar infrared spectra (Fig. 3b and c), with 1172 cm^{-1} representing the stretching vibration peak of C–N in the dA and dG, also with the 1612 cm^{-1} representing the stretching vibration peak of C═O in the dA and dG (Fig. 3d and e), indicating that the base were successfully binding to the surface of GCs.

3.2.3. *Elemental analysis*

To examine the alterations in the types and contents of elements in the prepared materials, the Vario ELIIII elemental analyzer was employed to analyze the carbon, hydrogen and nitrogen elements of GCs, GCs@dA and GCs@dG, respectively. The results were presented in Table 1. In comparison with GCs, the content of N in GCs@dA and GCs@dG increased significantly, while the carbon content of C decreased. The nitrogen came from the bases, which suggested that the DNA base was successfully grafted onto the surface of GCs.

3.2.4. *X-ray photoelectron spectroscopy*

The chemical composition of GCs and GCs@dG surfaces was analyzed using an X-ray photoelectron spectrometer. The results are presented in Fig. 4a. Both GCs and GCs@dG exhibited absorption peaks at 281.5 eV and 529 eV, corresponding to the absorption peaks of C1s and O1s. In comparison with the X-ray photoelectron spectroscopy of GCs, GCs@dA showed a stronger signal peak of N1s at 396 eV. The enhancement of this absorption peak indicated that the addition of purine increased the content of the nitrogen element, which was suggesting the success of the functionalized biochar preparation. This finding aligned with the results of elemental analysis above. The C1s spectra of GCs@dA demonstrated vast majority of C–C and C═O bonding states at 284.7 and 285.1 eV (Fig. 4b), which were supporting the successful preparation of typical carbon materials. And the O1s spectra in GCs@dA could be attributed to three peaks such as Quinone, C═O and C–OH bonding states at 531.7, 532.3 and 532.9 eV (Figs. 4c),[28] respectively, indicating the terriffc functionalities by heteroatom-doping of both GCs@dA.

3.3. *Selectivity adsorption capacity*

Various mechanisms contribute to the nephrotoxic adverse reactions caused by non-steroidal anti-inflammatory drugs, quinolone antibiotics and emodin, with the formation of adducts with DNA bases being one of the mechanism. This study employed the functionalized biochar to fill columns and verified the specific adsorption ability of GCs@dA and GCs@dG for nephrotoxic substances. For comparison, compounds with documented nephrotoxicity in the literature, as well as compounds not reported to have nephrotoxicity were both selected to determine at the same time. Nephrotoxic compounds included aristolochic acid I and II (AAI, AAII), ofloxacin (OFL), indomethacin (IND), and emodin (EMD), while penicillin sodium (PEN) was chosen as a compound without reported nephrotoxicity (the structure was shown in Fig. 5a). GCs@dA and GCs@dG were utilized to adsorb each compound, as depicted in Fig. 5b. The results indicated that the adsorption capacity of GCs@dG for aristolochic acid I and II were slightly higher than for other substrates, and the adsorption capacity of GCs@dG was slightly higher than that of GCs@dA. This suggested that the binding amount of the drug to guanine was higher than that to adenine. Furthermore, GCs@dA and GCs@dG demonstrated a certain recognition ability for compounds with nephrotoxic adverse reactions reported in the literature, such as ofloxacin, indomethacin and emodin. Notably, GCs@dA and GCs@dG exhibited no adsorption capacity for penicillin sodium, indicating that GCs@dA and GCs@dG possessed selectivity for nephrotoxic substances.

3.4. *Capture and analysis of suspicious nephrotoxic components in TCMs*

The GCs@dG was used as solid-phase extraction (SPE) medium to treat *Aristolochia debilis* Bge and *Aristolochia mollissima* Hance, the eluent was collected and analyzed under mobile phase 1 (the SPE process was shown in Fig. 6). As illustrated in Fig. 7, peaks corresponding to aristolochic acid I (40 min) and aristolochic acid II (33 min) appeared in the eluent of the two samples. This observation indicated a strong interaction force between AAs and the functionalized biochar. Given that aristolochic acids were well-known for their nephrotoxicity (one of the

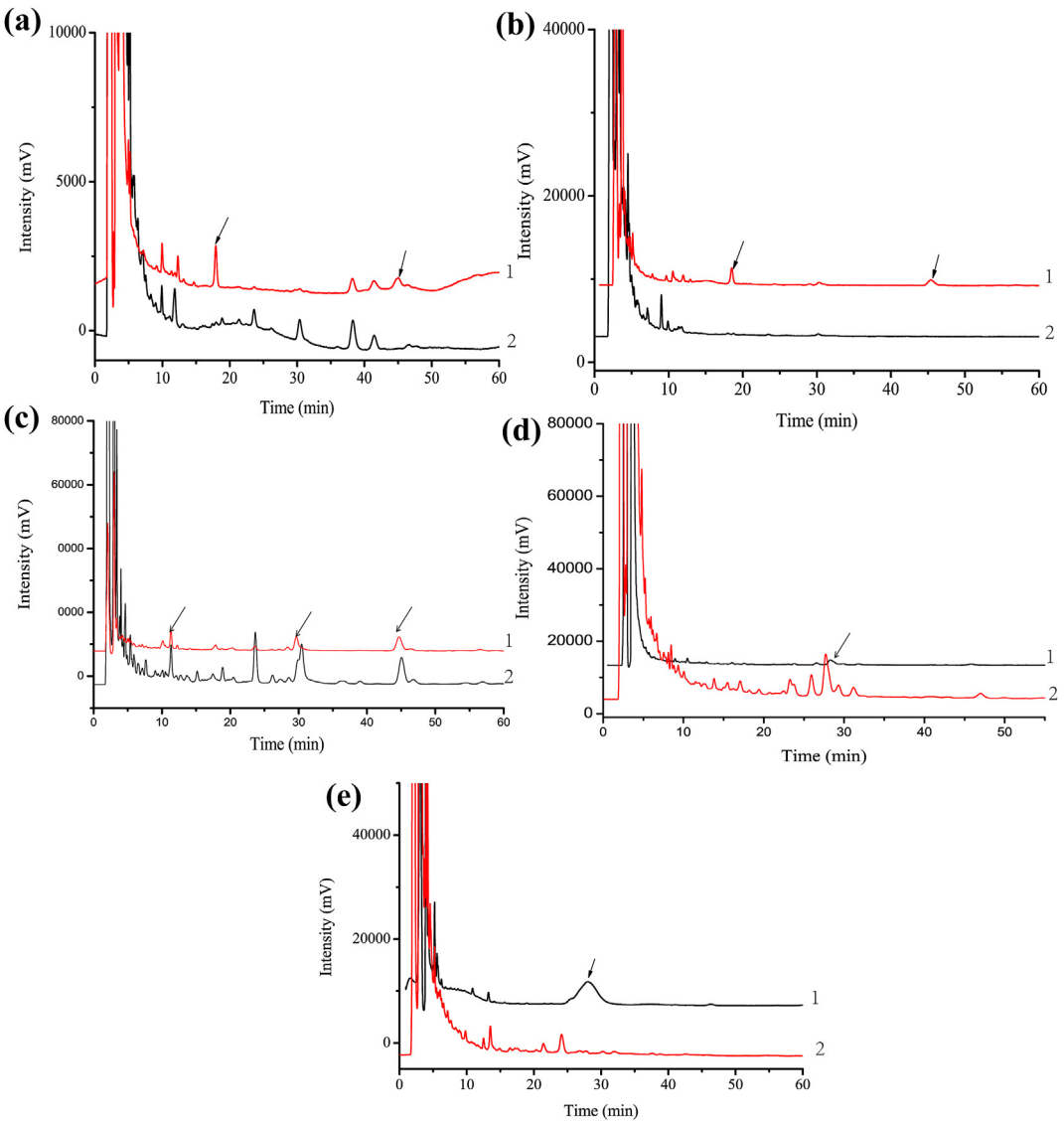

Fig. 8. The chromatogram of elutant of (a) *Radix aristolochiae* Fangji, (b) *Gastrodia elata* Bl. (c) *Asarum sieboldii* Miq. var. seoulense (d) *Coptis chinensis* Franch. (e) *Leonurus japonicus* Houtt. 1: after being adsorbed by GCs@dG; 2: before being adsorbed by GCs@dG; peaks marked with arrow: unknown suspected compounds.

mechanism was forming DNA-adducts), it suggested that guanine-functionalized biochar (GCs@dG) can effectively interact with toxic compounds in TCM with nephrotoxic effects. Additionally, some unknown compounds are still retained (as indicated by the arrows) in the SPE column, which still required further separation and identification.

This method was further employed for the analysis of suspected nephrotoxic substances in another five medicinal herbs, as depicted in Fig. 8. The herbs included *Gastrodia elata* Bl (Tianma), *Radix aristolochiae* S. Moore (Fangji), *Asarum sieboldii* Miq. var. Seoulense (Xixin), *Coptis chinensis* Franch. (Huanglian), and *Leonurus japonicus* Houtt. (Yimucao). In their elution solutions, some unknown peaks were retained strongly, such as strong peaks at 18 and 45 min in both Tianma and Fangji (Fig. 8a and b). However, the Huanglian sample did not show the accumulation of corresponding components after GCs@dG adsorption (Fig. 8d), indicating that no compounds were retained and enriched after being adsorbed by the purine functionalized biochar. Currently, there was no reports of Huanglian causing damage to renal function in clinical practice.[29] In Fig. 8c, three compounds were retained in the Xixin sample, which was commonly considered to be a nephrotoxic TCM.[30] The three compounds had the ability to bind with purine bases. Additionally, in Fig. 8e, there was a wide suspected peak in the Yimucao sample, indicating the presence of some suspected nephrotoxic substances. What's more, all these suspected peaks still need to be separated and identification. And its nephrotoxic mechanism also needed to explore, whether it was related to the formation of base adducts in vivo, in order to verify the specificity of the guanine-functionalized biochar.

In this study, a screening method for nephrotoxic substances in TCM was established by purine-functionalized biochar combined with SPE and HPLC (SPE-HPLC). However, there were certain limitations, including the HPLC mobile phase being specifically designed for the analysis of aristolochic acids in TCM samples. For known nephrotoxic compounds, there were challenges in retention on the HPLC column under the same condition. In the case of *Coptis chinensis* Franch, which was without reported nephrotoxic adverse reactions, and no retained ingredients were detected with SPE-HPLC. Similarly, for *Radix aristolochiae* Fangji and *Gastrodia elata* Bl., which was with reported potential nephrotoxicity, some components could be enriched with SPE-HPLC, but further separation, structural identification and even nephrotoxicity test were further needed for the suspected substances. The use of one mobile phase and wavelength specifically targeting aristolochic acids may not be representative for all nephrotoxic compounds. Additionally, other substances may undergo adsorption and retention but cannot be detected under the

given conditions. Therefore, it was necessary to combine other methods, such as mass spectrometry and nuclear magnetic resonance technology, for structural identification. Furthermore, considering the multiple theories on the mechanism of drug-induced nephrotoxicity, the formation of adducts between chemical components and DNA bases in the cell nucleus was just one aspect of nephrotoxicity. Due to the complex in vivo environment, this study had limitations in simulating this binding method in vitro. Therefore, the establishment of a screening model for nephrotoxic substances in TCM required further research.

4. Conclusions

In conclusion, functional biochar were developed using *Glycyrrhiza uralensis* Fisch and modified with purine bases. The physicochemical properties and apparent morphology of the resulting functional biochar were characterized and analyzed using SEM, FT-IR, XRS and elemental analysis. The adsorption selectivity of the functionalized biochar was studied subsequently, which revealed that functionalized biochar exhibited good adsorption capacity for compounds reported having nephrotoxicity, while it showed no adsorption capacity for compounds not reported having nephrotoxicity. The obtained functionalized materials were employed as filling solid-phase extraction adsorbents to screen and capture potential nephrotoxic substances in TCMs. The results demonstrated that the prepared biochar exhibited interactions with specific components in different TCMs. These work offered new ideas and methods for quickly capturing and large-scale screening nephrotoxic substances in TCM samples.

Data availability statement

The datasets generated during and/or analyzed during the current study are available from the corresponding author on reasonable request.

CRediT authorship contribution statement

Yanhui Ge: Writing – original draft, Supervision, Project administration, Methodology, Funding acquisition, Conceptualization. **Xinya Xu:** Writing – review & editing, Funding acquisition, Formal analysis. **Yuanru Zheng:** Writing – review & editing.

Declaration of competing interest

The authors declare that they have no known competing financial interests or personal relationships that could have appeared to influence the work reported in this paper.

Acknowledgements

This work was supported by the Scientific research funding of the First Affiliated Hospital of Guangdong Pharmaceutical University (KYQDJF202014), the Guangdong Basic and Applied Basic Research Foundation (SL2022A04J00538) and the Natural Science Foundation of Shaanxi Province (No. 2022JQ-821).

References

1. Chen WY, Luo H, Zhong ZF, et al. The safety of Chinese medicine: a systematic review of endogenous substances and exogenous residues. *Phytomedicine*. 2023;108:154534.
2. Jiang H, Li XY, Yang Fan, et al. The acute toxic effect of Chinese medicine Fuzi is exacerbated in kidney yang deficiency mice due to metabolic difference. *J Ethnopharmacol*. 2024;328:118036.
3. Gyamfi ET, Ackah W, Gore DB, et al. Bioaccessibility, exposure and risk assessment of potentially toxic elements and essential micronutrients in ayurvedic, traditional Chinese and Ghanaian medicines. *Biometals*. 2023;36:943–960.
4. Xiao YY, Liu RX, Zhang XY, et al. Analysis of cantharidin-induced kidney injury and the protective mechanism of resveratrol in mice determined by liquid chromatography/mass spectrometry-based metabonomics. J Appl Toxicol. doi.org/10.1002/jat.4596.
5. Chen YY, Tang LH, Wu MR, et al. A practical method for rapid discrimination of constituents in Psoraleae Fructus by UPLC-Q-Orbitrap MS. J Mass Spectrom. doi.org/10.1002/jms.4966.
6. Zhang LF, Lv RH, Huang WZ, et al. Establishment and evaluation of the stability of rat models of diabetic nepropathy induced by unilateral nephrectomy and streptozotocin injection. *Chin J Comp Med*. 2014;24:8–13.
7. Chen A, Sheu LF, Ho YS, et al. Experimental focal segmental glomerulosclerosis in mice. *Nephron*. 1998;78:440–452.
8. Yu XX, Li S, Tao JL, et al. Protective effects of BMP-7 against aristolochic acid-induced apoptosis of renal tubular epithelial cells. *Guangdong Med J*. 2011;32:821–823.
9. Badr AM, Al-kharashi LA, Attia H, et al. TLR4/inflammasomes cross-talk and pyroptosis contribute to n-acetyl cysteine and chlorogenic acid protection against cisplatin-induced nephrotoxicity. *Pharmaceuticals*. 2023;16:337.
10. Dogan T, Yildirim BA, Kapakin KAT, et al. Investigation of the effects of crocin on inflammation, oxidative stress, apoptosis, NF-kB, TLR-4 and Nrf-2/HO-1 pathways in gentamicin-induced nephrotoxicity in rats. *Environ Toxicol Pharmacol*. 2024;106:104374.
11. Ma J, Zhang W, He Y, et al. Clinical application of pyrrole-hemoglobin adducts as a biomarker of pyrrolizidine alkaloid exposure in humans. *Arch Toxicol*. 2021;95:759–765.
12. He XB, Xia QS, Shi Q, et al. Metabolism of carcinogenic pyrrolizidine alkaloids and pyrrolizidine alkaloid N-oxides by rat primary hepatocytes generate the same characteristic DHP-DNA adducts. *J Env Sci Heal C-Tox*. 2021;39:357–372.
13. Hernandez-Castillo C, Termini J, Shuck S. DNA adducts as biomarkers to predict, prevent, and diagnose disease-application of analytical chemistry to clinical investigations. *Chem Res Toxicol*. 2020;33:286–307.
14. Zhao XP, Guo M, Zhang BL. An approach to screen nephrotoxic components in traditional Chinese medicine based on fluorescent probe and HK-2 cells and its application. *China J Materia Medica*. 2013;38(10):1577.
15. Guan Y, Su SB. Bio-chip technology and its application development on the traditional Chinese medicine research. *Chin J Tradit Chin Med*. 2012;27(2):422–425.
16. He M, Liang XX, Jiang BP, et al. Regulated gene expression profile of cyclovirobuxine-D in rat renal by gen chip technique. *Chin J Exp Tradit Med Formulae*. 2013;19(10):286–290.
17. Wang M, Liu CX, Dong RR, et al. Safety evaluation of Chinese medicine injections with a cell imaging-based multiparametric-assay revealed a critical involvement of mitochondrial function in hepatotoxicity. *Evid Based Complement Alternat Med*. 2015;2015:1–13.
18. Liu RL, Yu P, Luo ZM, et al. Single-helix carbon microcoils prepared via Fe(III)-osmotically induced shape transformation of zucchini (*Cucurbita pepo* L.) for enhanced adsorption and antibacterial activities. *Chem Eng J*. 2017;315:437–447.
19. Xu XY, Guo PQ, Shu H, et al. Preparation of biocompatible molecularly imprinted film on biowastederived magnetic pomegranate rind carbon for protein recognition in biological sample. *Mater Sci Eng C*. 2020;115:111063.
20. Shu H, Ge YH, Xu XY, et al. Hybrid-type carbon microcoil-chitosan composite for selective extraction of aristolochic acid I from Aristolochiaceae medicinal plants. *J Chromatogr A*. 2018;1561:13–19.
21. Ge YH, Shu H, Xu XY, et al. Combined magnetic porous molecularly imprinted polymers and deep eutectic solvents for efficient and selective extraction of aristolochic acid I and II from rat urine. *Mater Sci Eng C*. 2019;97:650–657.
22. Ge YH, Zhao SC, Yuan BY, et al. In-situ growth of metal coordination-synergistic imprinted polymer onto shrimp shell-derived magnetic FeNi biochar for specific recognition of monocrotaline in herbal medicine. *Mater Today Sustain*. 2023;24:100599.
23. Tian JZ, Liu CY, Wang LM, et al. Study on the difference and correlation between the contents and toxicity of aristolochic acid analogues in *Aristolochia* plants. *J Ethnopharmacol*. 2023;315:116568.
24. Papadakis JA, Samonis G, Marakis S, et al. Efficacy of amikacin, ofloxacin, pefloxacin, ciprofloxacin, enoxacin and fleroxacin in experimental left-sided Pseudomonas aeruginosa endocarditis. *Chemtheropy*. 2000;46:116–121.
25. Yen NTH, Oh JH, Anh NTV, et al. Systems-level multi-omics characterization provides novel molecular insights into indomethacin toxicity. *Chem Biol Interact*. 2023;375:110430.
26. Yang Z, Qin W, Chen D, et al. In vitro study of emodin-induced nephrotoxicity in human renal glomerular endothelial cells on a microfluidic chip. *Biocell*. 2024;47:125.
27. Ge YH, Guo PQ, Xu XY, et al. Selective analysis of aristolochic acid I in herb medicines by dummy molecularly imprinted solid-phase extraction and HPLC. *J Separ Sci*. 2017;40(13):2791–2799.
28. Liu YJ, Liu SL, Tian Y, et al. Dual/triple template-induced evolved emulsion for controllable construction of anisotropic carbon nanoparticles from concave to convex. *Adv Mater*. 2023;35:2210963.
29. Su GY, Wang HF Wang, Gao YX, et al. ^{1}H-NMR-based metabonomics of the protective effect of coptis chinensis and berberine on cinnabar-induced hepatotoxicity and nephrotoxicity in rats. *Molecules*. 2017;22(11):1855.
30. Liu MT, Wang LM, Qin SS, et al. Long-term oral administration of *Asarum heterotropoides* f. mandshuricum (Maxim.) Kitag. decoction and its aristolochic acid analogs do not cause renal toxicity in mice. *J Ethnopharmacol*. 2023;307:116.